

Supplementary Information for

The cytoplasmic synthesis and coupled membrane translocation of eukaryotic polyphosphate by signal-activated VTC complex

Zeyuan Guan[#], Juan Chen[#], Ruiwen Liu[#], Yanke Chen[#], Qiong Xing[#], Zhangmeng Du,
Meng Cheng, Jianjian Hu, Wenhui Zhang, Wencong Mei¹, Beijing Wan¹, Qiang Wang,
Jie Zhang, Peng Cheng, Huanyu Cai, Jianbo Cao, Delin Zhang, Junjie Yan, Ping Yin,
Michael Hothorn, Zhu Liu^{*}

[#]These authors contributed equally to this work.

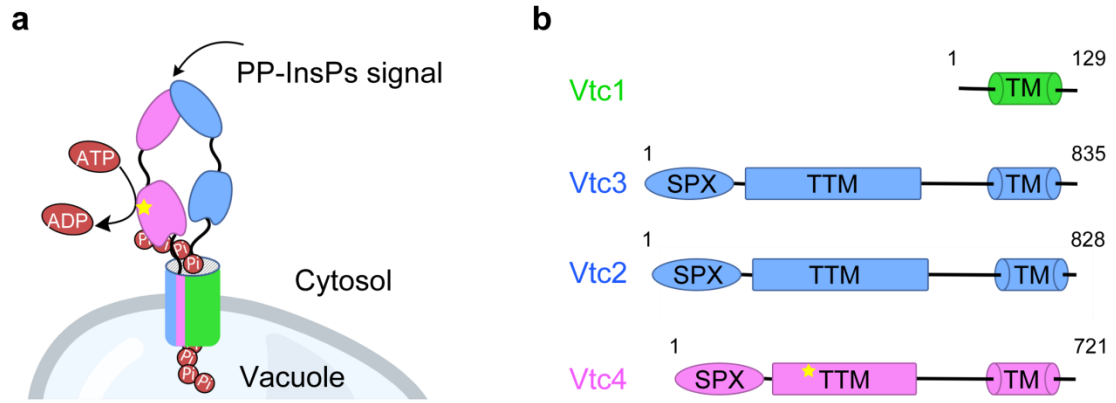
^{*}Corresponding author: liuzhu@hzau.edu.cn (Z. L.).

This PDF file includes:

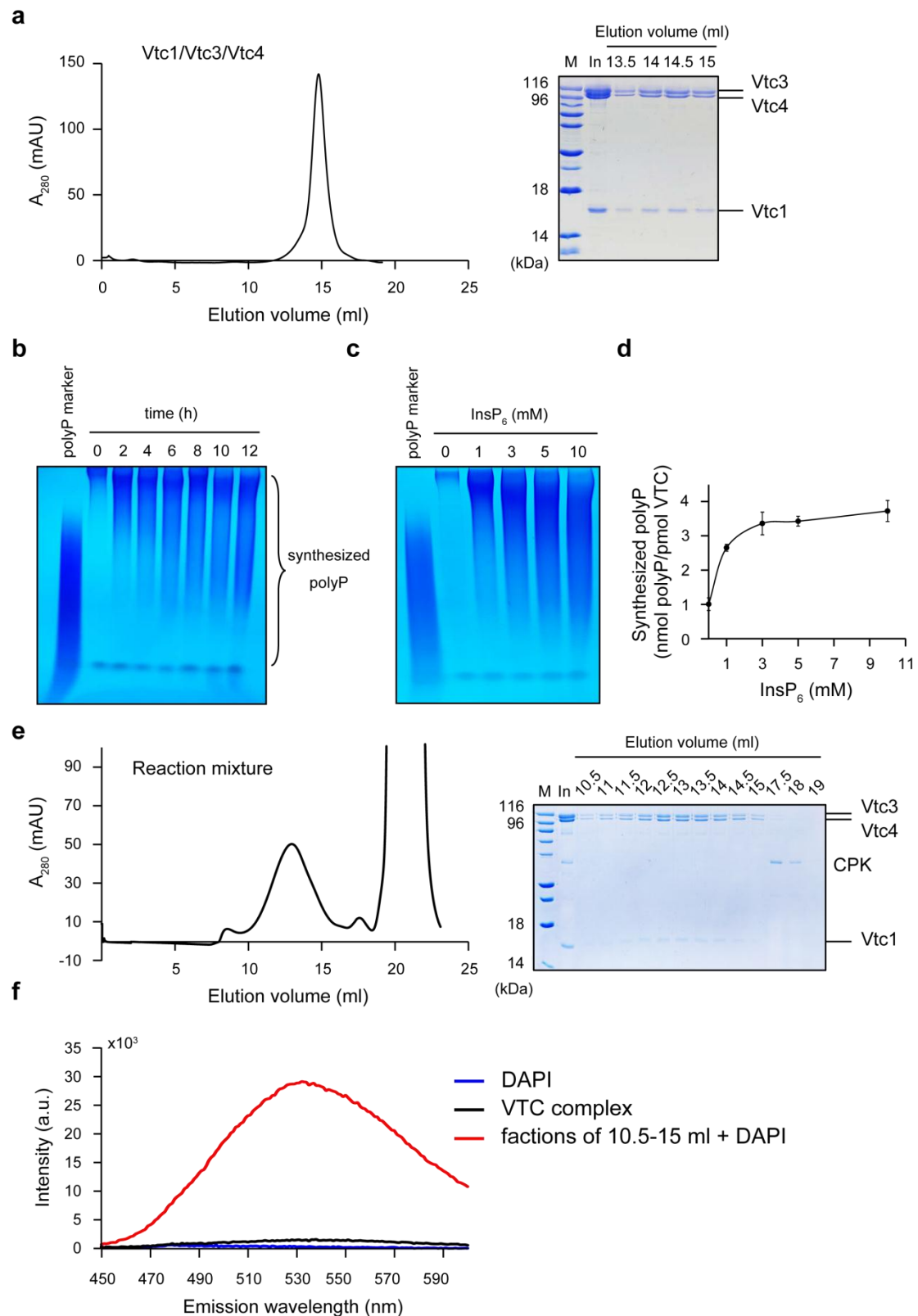
Supplementary Figs. 1-15

Supplementary Tables 1-3

References

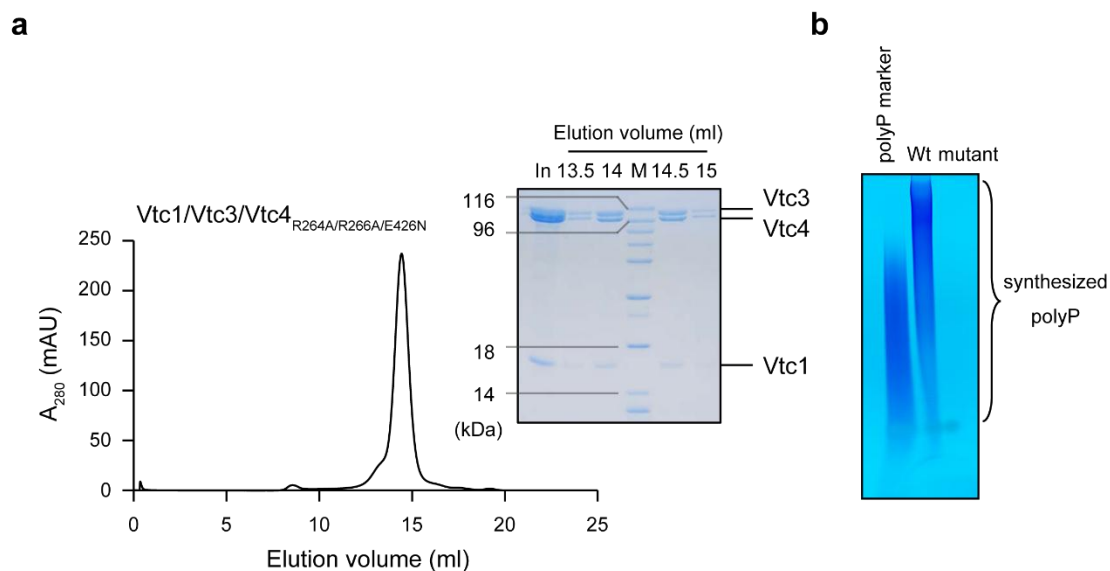


Supplementary Figure 1. (a) Schematic working model and (b) domain architectures of Vtc subunits. TM, trans-membrane domain; SPX, SYG1/Pho81/XPR1 domain; TTM, triphosphate tunnel metalloenzyme domain. A yellow star indicates the catalytic polymerase domain for polyP synthesis.



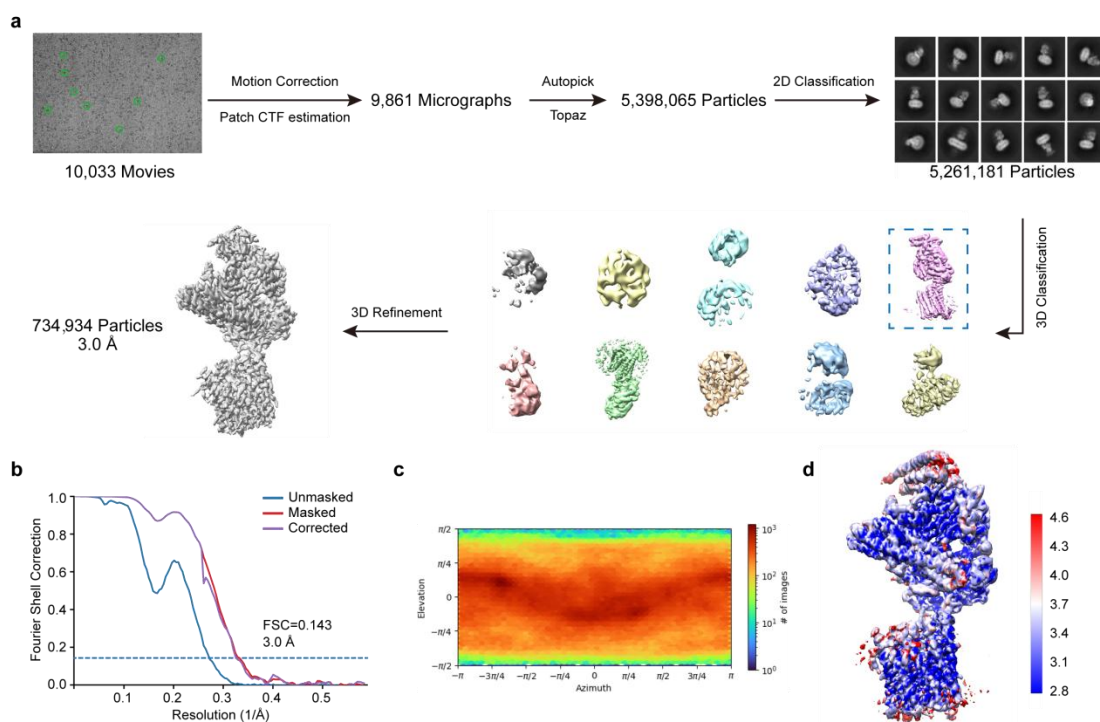
Supplementary Figure 2. Purification of the VTC complex and polyP activity assay. (a) Representative size-exclusion chromatography (SEC) purification of the Vtc1/Vtc3/Vtc4 complex in the absence of InsP₆. In, input sample before SEC step. Source data are provided as a Source Data file. The experiments were repeated more than five times independently with similar results. (b) TBE-PAGE visualization of polyP synthesized by the Vtc1/Vtc3/Vtc4 complex. The reactions

were performed with required times before stopped. 5 μM protein complex and 10 mM InsP_6 were used for each reaction. A commercial polyP with an average chain length of 60 residues (polyP60) was used as the marker. Source data are provided as a Source Data file. The experiments were repeated three times independently with similar results. (c) TBE-PAGE visualization of polyP synthesized by Vtc1/Vtc3/Vtc4 complex. The reactions were performed at required InsP_6 concentrations. 5 μM protein complex were used and reactions were performed for 4 hours. Source data are provided as a Source Data file. The experiments were repeated three times independently with similar results. (d) Quantification of the produced polyP from (c) using DAPI-based measurement¹. PolyP60 was used for assay calibration. Data from three measurements were averaged, and the error indicates SD. Source data are provided as a Source Data file. (e) SEC analysis of the reaction mixture. 5 μM protein complex and 10 mM InsP_6 were used and the reaction of polyP synthesis was performed for 2 hours. Then the reaction mixture was subjected onto SEC. Fractions of eluent were visualized on SDS-PAGE gel. In, input reaction mixture before SEC step. CPK, creatine phosphokinase used in the reaction. Source data are provided as a Source Data file. The experiments were repeated two times independently with similar results. (f) DAPI detecting the retained polyP in the collected SEC fractions of the reaction mixture. Fractions of VTC at 10.5-15 ml elution volume of (e) were collected and concentrated for the DAPI detection. 0.2 μM concentrated protein fractions and 10 μM DAPI were used for the fluorescent detection. As controls, 0.2 μM purified VTC complex and 10 μM DAPI were used, respectively. The experiments were repeated two times independently with similar results.

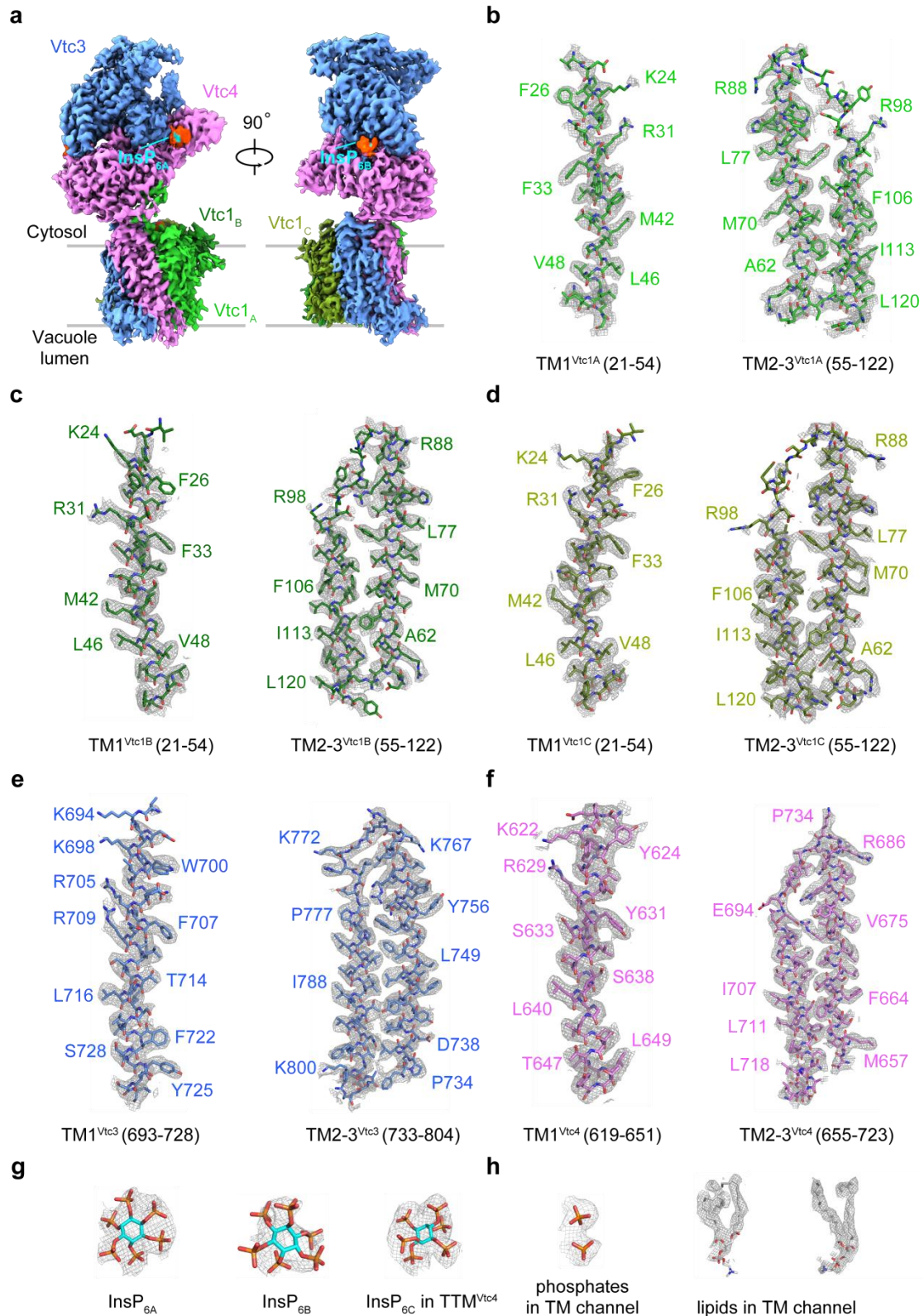


Supplementary Figure 3. Purification of the VTC complex for cryo-EM analysis. (a) Representative SEC purification of the Vtc1/Vtc3/Vtc4 complex carrying three point mutations on Vtc4 (Vtc1/Vtc3/Vtc4_{R264A/R266A/E426N}) in the presence of 1 mM InsP_6 . In, input sample before SEC step. Fractions of Vtc1/Vtc3/Vtc4_{R264A/R266A/E426N} at 14 and 14.5 ml elution volume were pooled for cryo-EM analysis. Source data are provided as a Source Data file. The experiments were repeated more than five times independently with similar results. (b) TBE-PAGE visualization of polyP synthesized by Vtc1/Vtc3/Vtc4 (Wt) and Vtc1/Vtc3/Vtc4_{R264A/R266A/E426N}

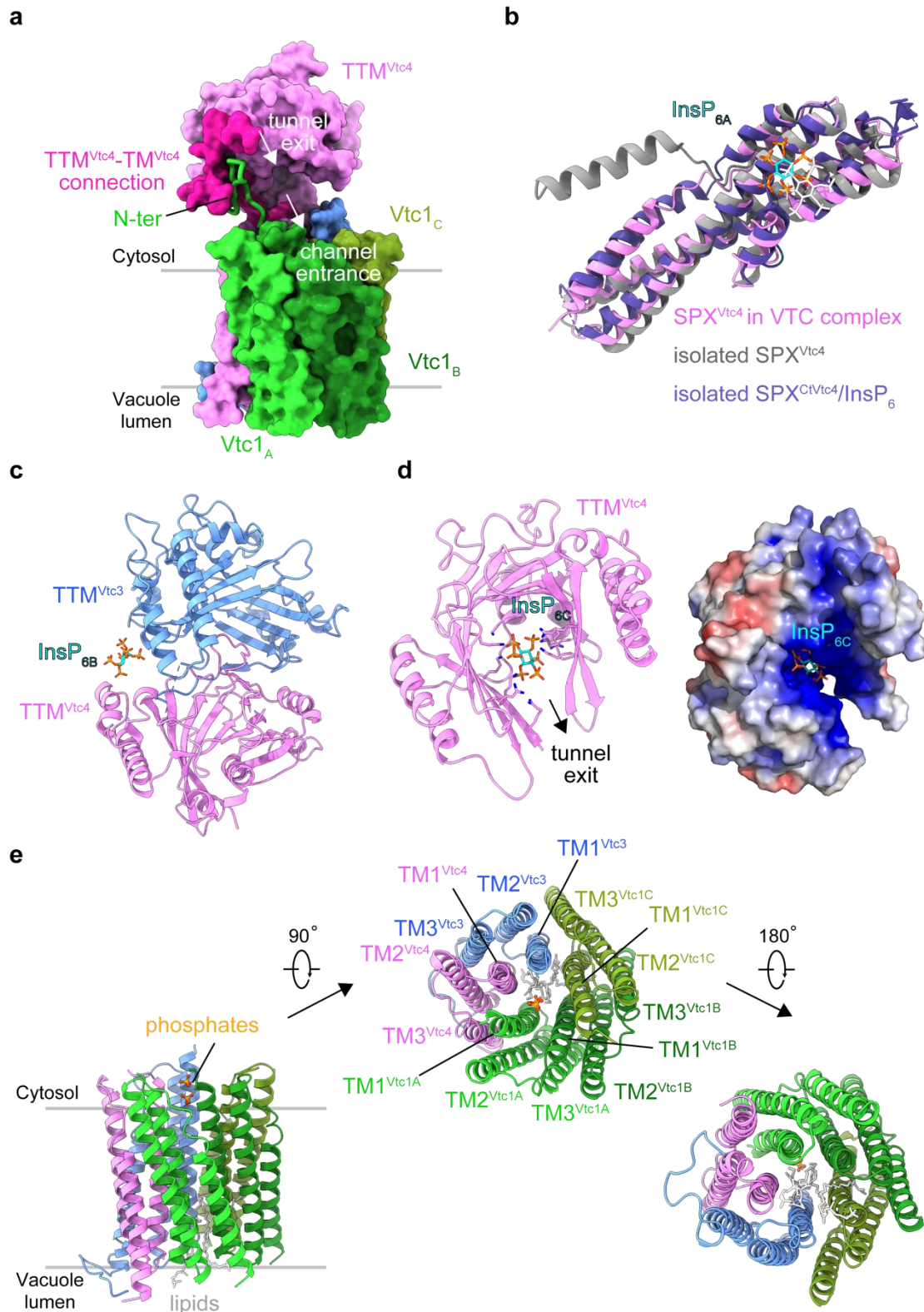
(mutant) complex. 5 μM protein complex and 10 mM InsP_6 were used, and reactions were performed for 4 hours. Source data are provided as a Source Data file. The experiments were repeated three times independently with similar results. Blocking VTC activity via three amino-acid substitutions of known catalytic residues in TTM^{VTC4} (R264A/R266A/E426N)², allowed us to collect high-quality cryo-EM micrographs for single particle analysis.



Supplementary Figure 4. Cryo-EM structural analysis of the VTC complex. (a) Flow chart for EM data processing. 3D refinement generated a 3.0 Å map of $\text{Vtc1/Vtc3/Vtc4}_{\text{R264A/R266A/E426N}}$ in complex with InsP_6 . Typical particles of the complex are marked by green circles in the representative electron micrograph. Details can be found in Methods. (b) Gold-standard Fourier shell correlation (FSC) curve for the VTC map refinement. Average resolution of this map is estimated to be 3.0 Å. (c) Angular distribution of the particles used for reconstruction. (d) Sharpened map of the complex, colored according to local resolution.

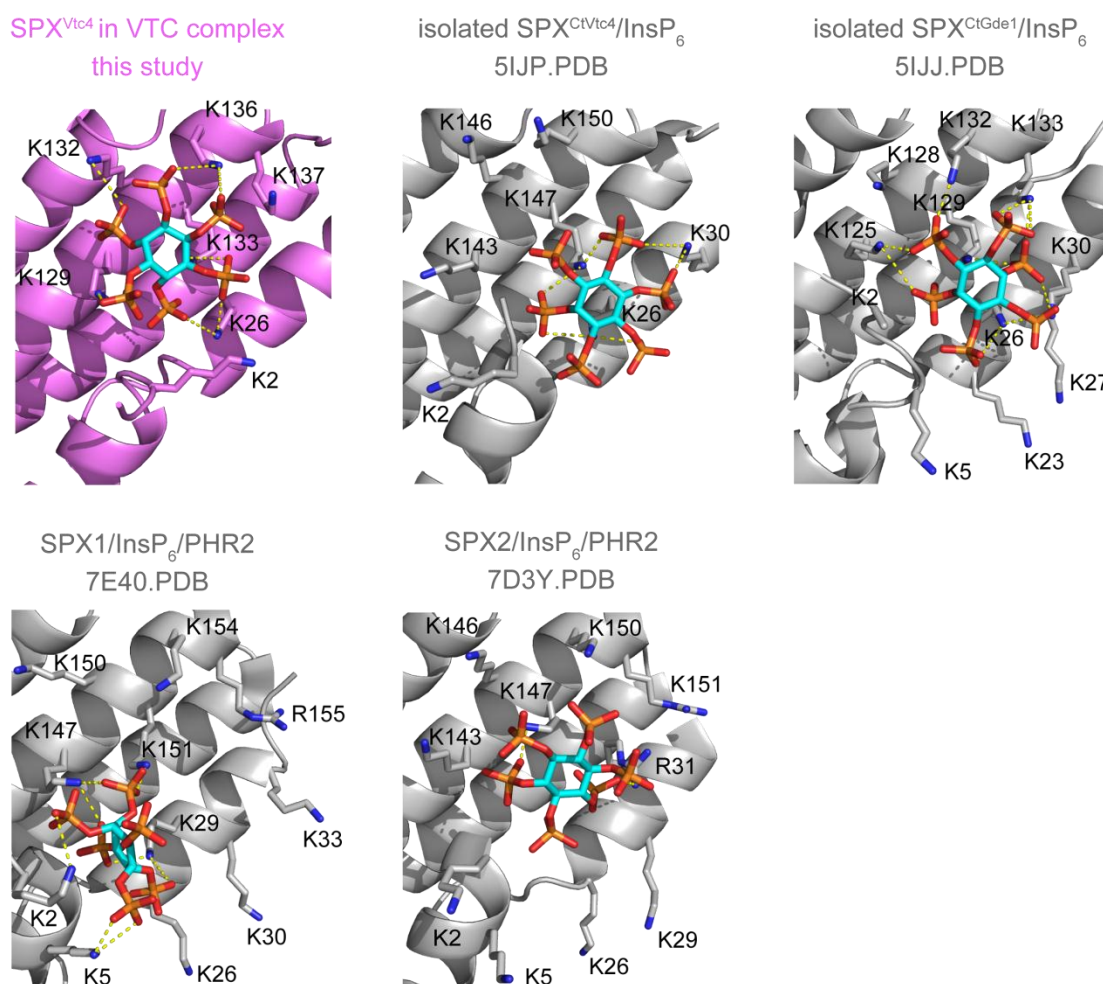


Supplementary Figure 5. Representative EM densities. (a) The EM density map of the Vtc1/Vtc3/Vtc4_{R264A/R266A/E426N} in complex with InsP₆. (b-f) EM density maps for the indicated trans-membrane helices in the TM region of the complex. (g) and (h), EM density maps for the indicated molecules observed in the complex. All the densities were contoured at 5.5 σ and visualized using PyMol 2.4.1.

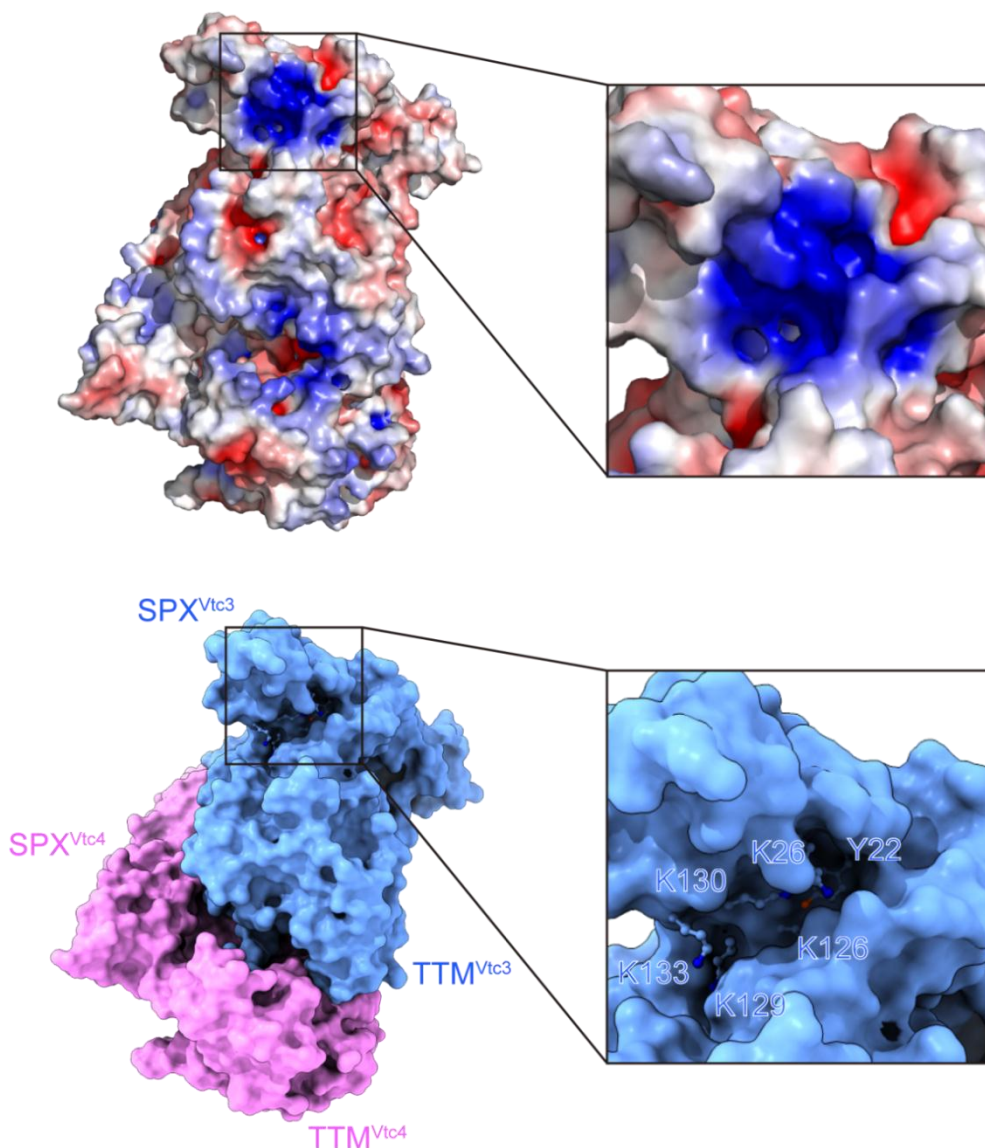


Supplementary Figure 6. Structural segments of the InsP₆-activated VTC complex. (a) Orientation between the catalytic TTM^{Vtc4} domain and the assembled trans-membrane channel. The connection between TTM^{Vtc4} and TM^{Vtc4} (residues 472-618) is represented in magenta surface. The N-terminus of Vtc1_A protomer (residues 1-21) is shown in cartoon representation. (b) Structure comparison between InsP₆-bound SPX^{Vtc4} in our entire yeast VTC complex and

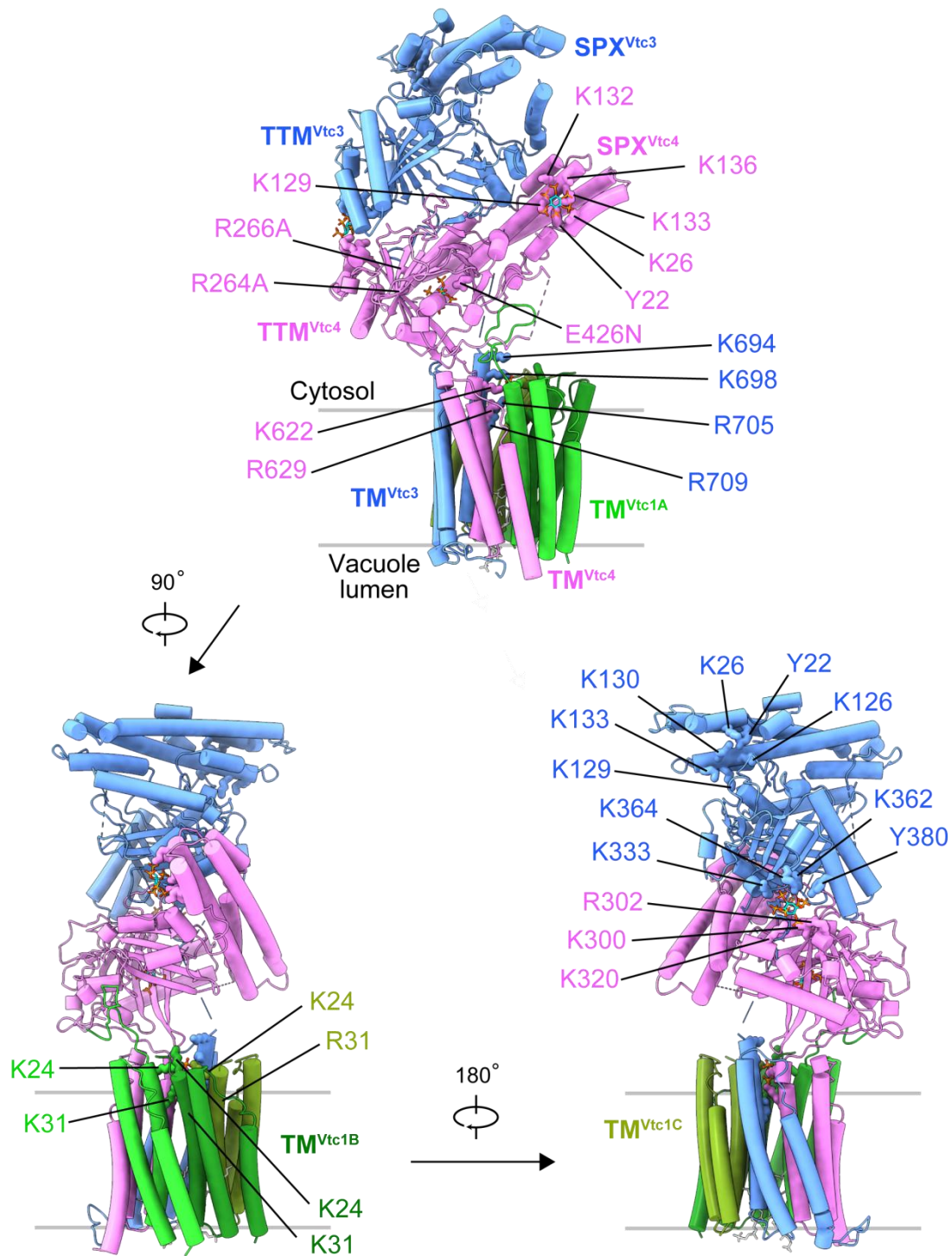
previously reported isolated SPX fragments. The structure of isolated yeast SPX^{Vtc4} fragment (5IIT.PDB)³ and isolated *Chaetomium thermophilum* SPX^{CtVtc4} fragment in complex with InsP₆ (5IJP.PDB)³ are colored in gray and purple cartoon representations, respectively. InsP₆ of 5IJP.PDB is shown in white stick representation. (c) The second InsP₆ molecule (InsP_{6B}) binds simultaneously to TTM^{Vtc3} and TTM^{Vtc4}. (d) The third InsP₆ molecule (InsP_{6C}) appears in the positively charged tunnel of TTM^{Vtc4}. Positive residues in inner wall of the tunnel are shown as stick in the cartoon representation of TTM^{Vtc4}. Electrostatic surface is represented in the same perspective, colored in terms of electrostatic potential and displayed in a scale from red (-5 kT/e) to blue (+5 kT/e). (e) Molecules of two phosphates and two lipids occupy in the cytoplasmic side and luminal side of trans-membrane channel, respectively. Phosphates and lipids are shown in stick representations.



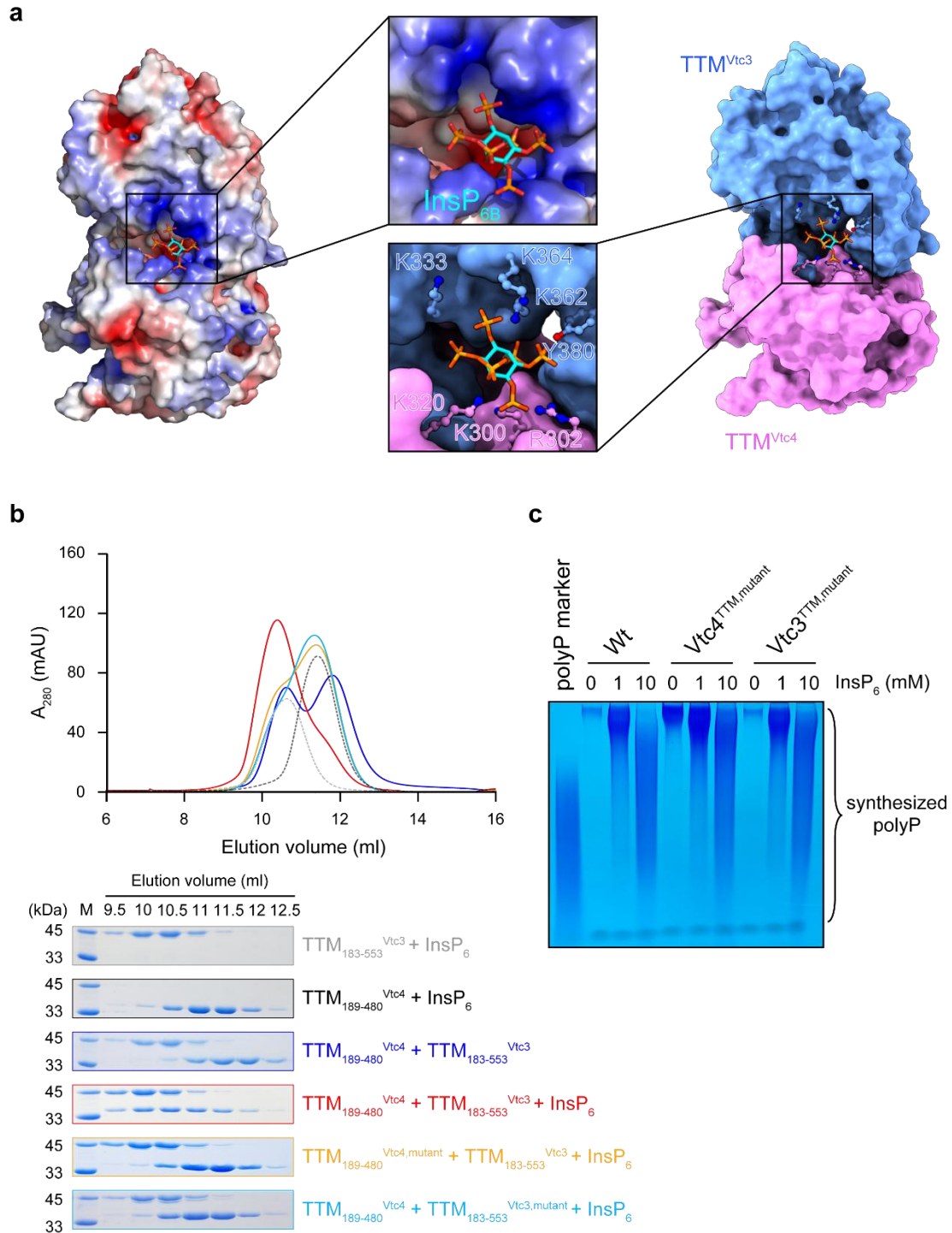
Supplementary Figure 7. Coordination of InsP₆ bound to different SPX domain-containing proteins. All SPX domains (depicted as cartoon diagrams) are shown in the same orientations. Other proteins in the complex structures have been omitted for clarity. Positively charged residues constituting the basic surface patch in SPX proteins are shown in stick representation. Yellow dashed lines indicate the coordination of InsP₆.



Supplementary Figure 8. Electrostatic surface (upper panel) and molecular surface (lower panel) representation of SPX and TTM domains in the InsP_6 -activated VTC complex. They are displayed in the same perspective. Electrostatic potential is calculated with the APBS plugin in PyMOL, colored and displayed in a scale from red (-5 kT/e) to blue ($+5 \text{ kT/e}$). SPX^{Vtc3} PBC (Y22, K26, K130) and KSC (K126, K129, K133) residues are shown in stick representation.

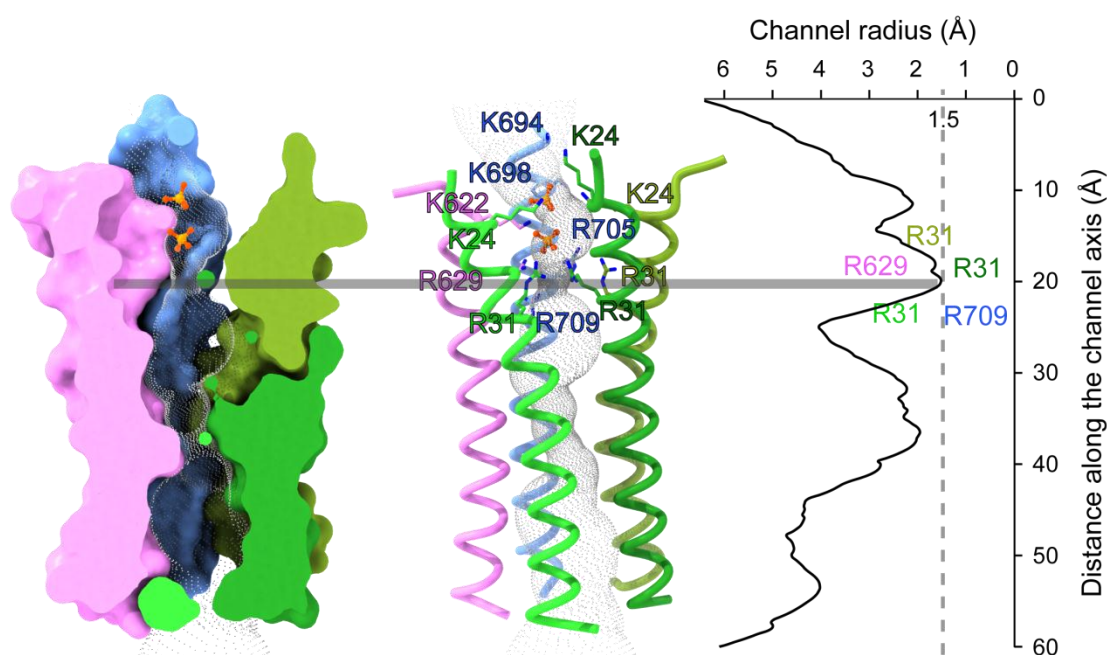


Supplementary Figure 9. Sites of point mutations used in this study. The VTC complex structure is presented in same scheme as Fig. 1 in the main text. Mutations of subunit Vtc4 R264A/R266A/E426N were used for structure determination, and others were used for function studies.

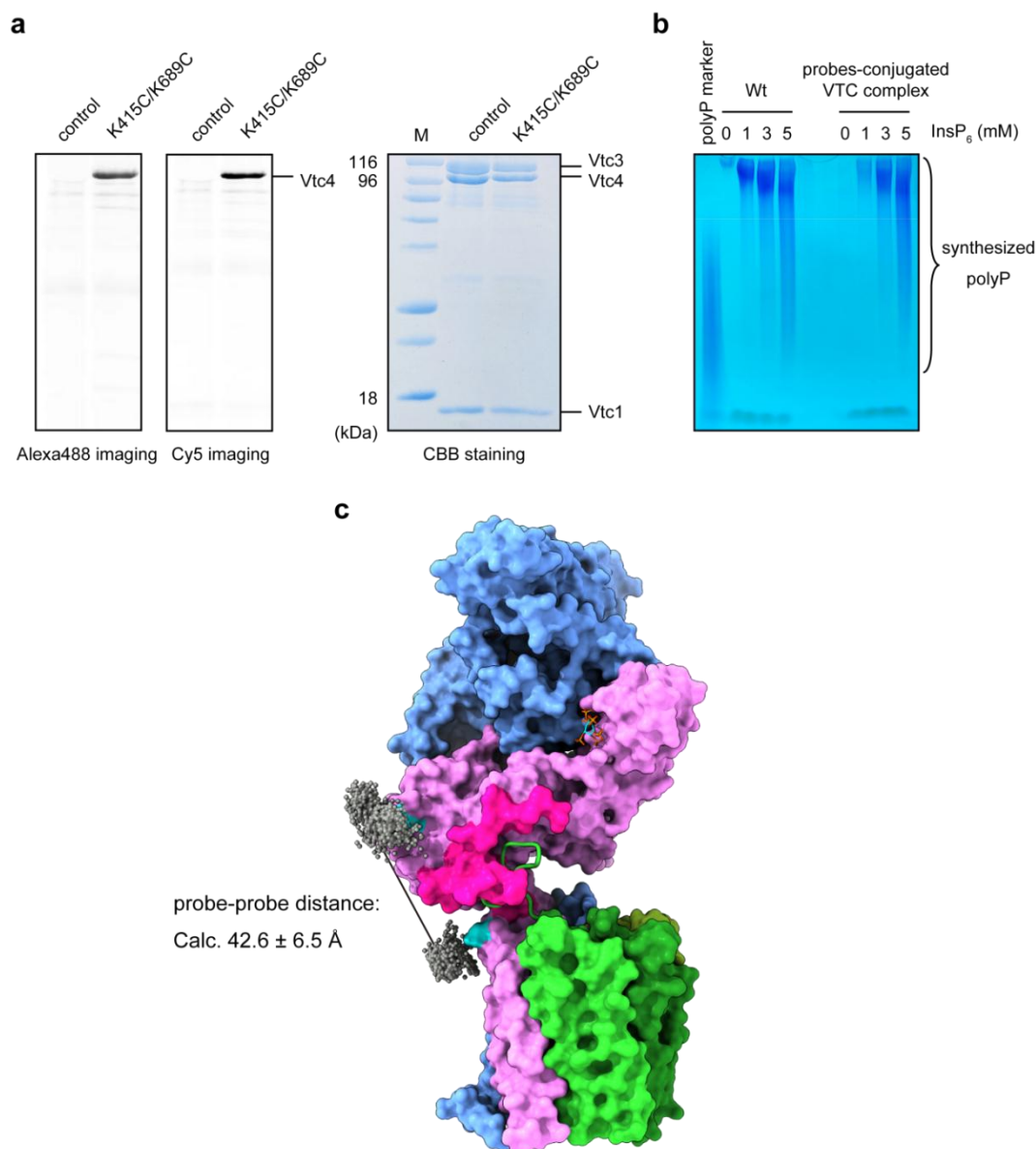


Supplementary Figure 10. An InsP_6 molecule is coordinated between TTM^{Vtc4} and TTM^{Vtc3} in the InsP_6 -activated VTC complex. (a) InsP_6 binds to a positively charged cleft that is formed by TTM^{Vtc4} and TTM^{Vtc3} . The Electrostatic surface (left) and molecular surface (right) representation of TTM^{Vtc3} and TTM^{Vtc4} domains are displayed in the same perspective. Electrostatic potential is calculated with the APBS plugin in PyMOL, colored and displayed in a scale from red (-5 kT/e) to blue ($+5$ kT/e). Residues for InsP_6 coordination are shown in stick representation. (b) InsP_6 promotes TTM^{Vtc4} - TTM^{Vtc3} association. The isolated $\text{TTM}_{189-480}^{\text{Vtc4}}$ and $\text{TTM}_{183-553}^{\text{Vtc3}}$ contain residues 189-480 and residues 183-553, respectively. $\text{TTM}_{189-480}^{\text{Vtc4,mutant}}$ and $\text{TTM}_{183-553}^{\text{Vtc3,mutant}}$ carry K300A/R302A/K320A and K333A/K362A/K364A/Y380F point

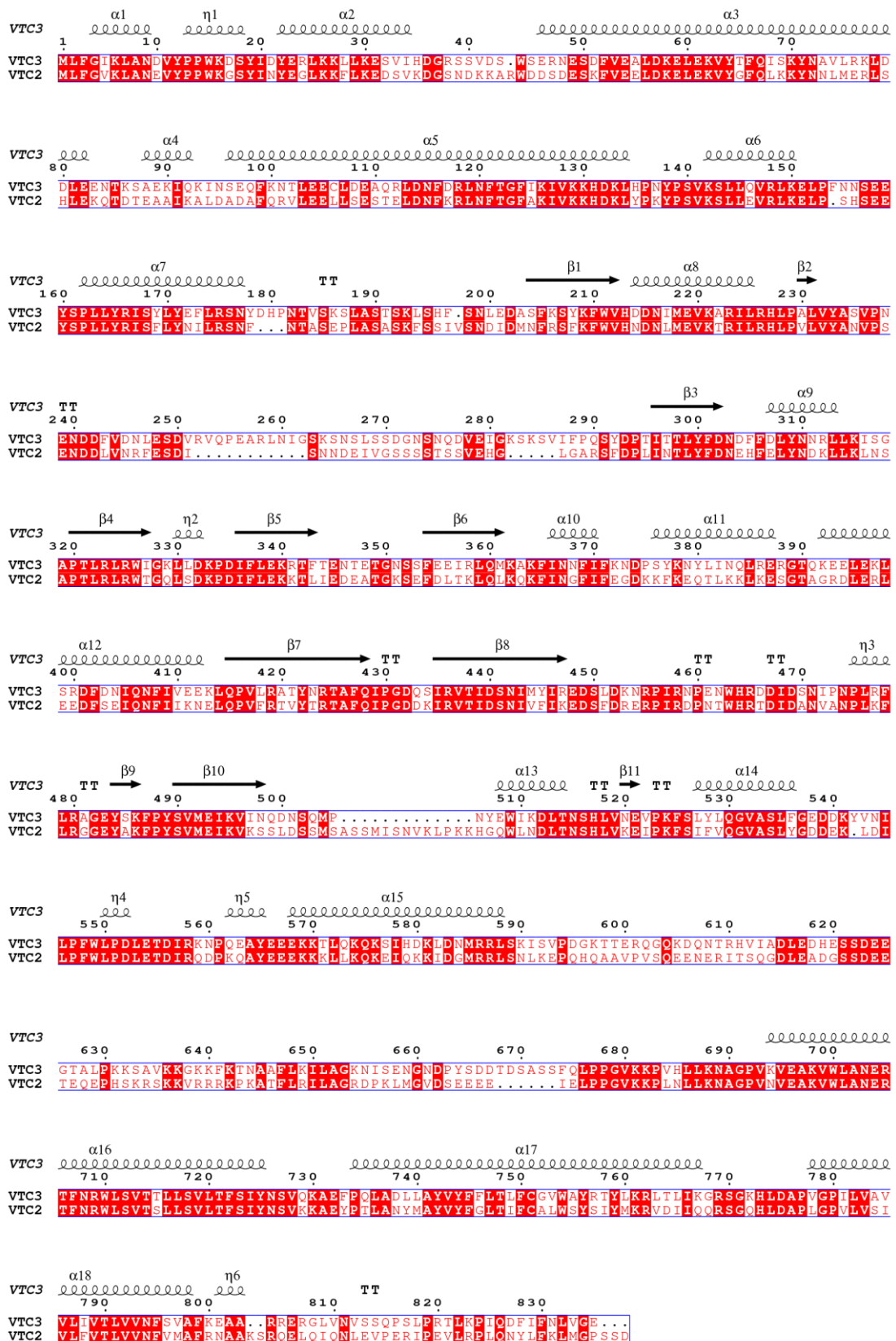
mutations, respectively. (Top) Gel filtration profiles of $\text{TTM}_{183-553}^{\text{Vtc3}}$, $\text{TTM}_{189-480}^{\text{Vtc4}}$, $\text{TTM}_{189-480}^{\text{Vtc4}}$ and $\text{TTM}_{183-553}^{\text{Vtc3}}$ mixture, $\text{TTM}_{189-480}^{\text{Vtc4,mutant}}$ and $\text{TTM}_{183-553}^{\text{Vtc3}}$ mixture, $\text{TTM}_{189-480}^{\text{Vtc4}}$ and $\text{TTM}_{183-553}^{\text{Vtc3,mutant}}$ mixture in the presence of 1 mM InsP_6 , and $\text{TTM}_{189-480}^{\text{Vtc4}}$ and $\text{TTM}_{183-553}^{\text{Vtc3}}$ mixture in the absence of InsP_6 were colored in gray, black, red, yellow, cyan and blue, respectively. (Bottom) Coomassie-blue stained SDS-PAGE gels of each peak fractions. About 25 μM protein or 50 μM mixture (25 μM for each) were used for the SEC assay. Source data are provided as a Source Data file. The experiments were repeated two times independently with similar results. (c) Assay of VTC-catalyzed polyP synthesis. Cleft mutations in either TTM^{Vtc4} ($\text{Vtc4}^{\text{TTM,mutant}}$, $\text{Vtc1/Vtc3/Vtc4}_{\text{K300A/R302A/K320A}}$) or TTM^{Vtc3} ($\text{Vtc3}^{\text{TTM,mutant}}$, $\text{Vtc1/Vtc3}_{\text{K333A/K362A/K364A/Y380F/Vtc4}}$) had little impact on InsP_6 -stimulated polyP synthesis by VTC complex. 5 μM protein complex were used and reactions were performed at required InsP_6 concentrations for 4 hours. Source data are provided as a Source Data file. The experiments were repeated two times independently with similar results.



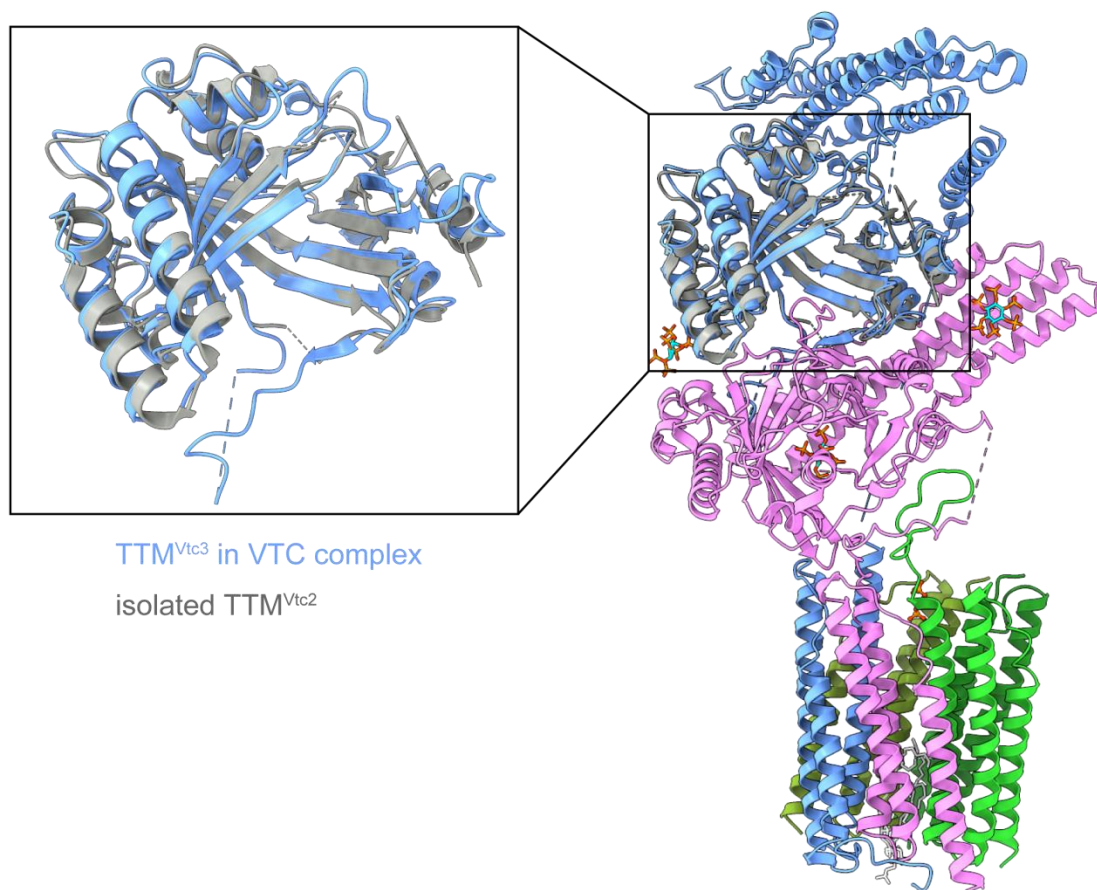
Supplementary Figure 11. Channel path analysis. Surface representation with half-cut view (left) and cartoon representation (middle) of the TM1s-assembled trans-membrane channel. Basic residues of the five TM1s in the interior wall and the occupied phosphates are shown in stick representations. Channel path (gray dots representation) and channel radius (right) was calculated using HOLE⁴ for the VTC complex structure, without the inside phosphates and lipids. The dashed line indicates the narrowest position of the channel, that is surrounded by R31 of TM1^{Vtc1} , R709 of TM1^{Vtc3} , and R629 of TM1^{Vtc4} , with a radius of 1.5 Å. The VTC complex structure is colored in same scheme as Fig. 4b in the main text.



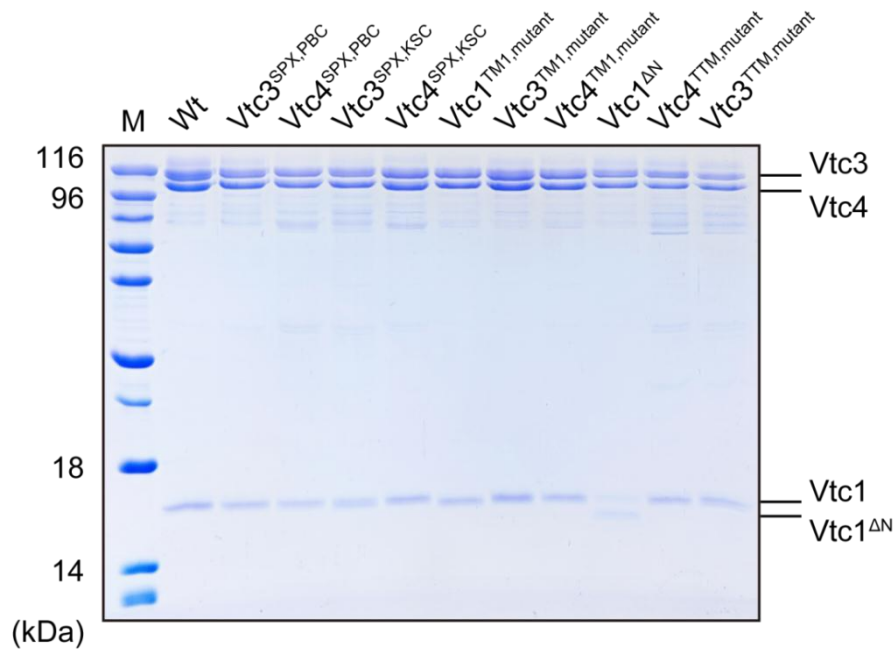
Supplementary Figure 12. Sample used for smFRET analysis. (a) Specifically labeling of the VTC complex. Control, all intrinsic cysteine in the Vtc1/Vtc3/Vtc4 complex were substituted; K415C/K689C, substituting all intrinsic cysteine in the VTC complex and further generating additional cysteine to K415 and K689 in the Vtc4 subunit. The images of Alexa488 and Cy5 on SDS-PAGE gel were obtained using Typhoon, and the gel was further stained using coomassie brilliant blue (CBB). Source data are provided as a Source Data file. The experiments were repeated three times independently with similar results. (b) Assay of VTC-catalyzed polyP synthesis. Wt, the Vtc1/Vtc3/Vtc4 wild-type complex; probes-conjugated VTC complex, the sample used for smFRET analysis. 5 μM protein complex were used and reactions were performed at required InsP₆ concentrations for 3 hours. Source data are provided as a Source Data file. The experiments were repeated three times independently with similar results. (c) Calculated average distance between conjugated probes. The accessible volume of conjugated probes on the structure were sampled using Xplor-NIH⁵ (See Methods for details). The geometric centers of the two chromophores were represented with gray spheres, and the average distance between them is $42.6 \pm 6.5 \text{ \AA}$. The VTC complex structure is colored in same scheme as Fig. 5c in the main text.



Supplementary Figure 13. Sequence alignment. The sequence of yeast Vtc3 subunit is aligned with Vtc2. Structure-based alignment was performed by ESPrpt (3.0). The sequence identity is indicated by white letters against a red background, and the sequence of a similarity over 90% is indicated by red letters. The secondary elements of Vtc3 are labeled at the top of the alignment.



Supplementary Figure 14. Structure comparison. The structure of isolated TTM^{Vtc2} fragment² (3G30.PDB) is superposed to the TTM^{Vtc3} domain in the InsP₆-activated Vtc1/Vtc3/Vtc4 complex structure, with an overall RMSD of 1.03 Å.



Supplementary Figure 15. Samples used for the assay of VTC-catalyzed polyP synthesis in this study. Wt, Vtc1/Vtc3/Vtc4; Vtc3^{SPX,PBC}, Vtc1/Vtc3^{Y22F/K26A/K130A}/Vtc4; Vtc4^{SPX,PBC}, Vtc1/Vtc3/Vtc4^{Y22F/K26A/K133A}; Vtc3^{SPX,KSC}, Vtc1/Vtc3^{K126A/K129A/K133A}/Vtc4; Vtc4^{SPX,KSC}, Vtc1/Vtc3/Vtc4^{K129A/K132A/K136A}; Vtc1^{TM1,mutant}, Vtc1^{K24A/R31A}/Vtc3/Vtc4; Vtc3^{TM1,mutant}, Vtc1/Vtc3^{K694A/K698A/R705A/R709A}/Vtc4; Vtc4^{TM1,mutant}, Vtc1/Vtc3/Vtc4^{K622A/R629A}; Vtc1^{ΔN}, Vtc1^{Δ1-21}/Vtc3/Vtc4; Vtc4^{TTM,mutant}, Vtc1/Vtc3/Vtc4^{K300A/R302A/K320A}; Vtc3^{TTM,mutant}, Vtc1/Vtc3^{K333A/K362A/K364A/Y380F}/Vtc4. Source data are provided as a Source Data file. The experiments were repeated two times independently with similar results.

Supplementary Table 1.

Cryo-EM data collection and refinement statistics

	PDB: 7YTJ EMBD: EMD- 34090
Data collection and processing	
Microscope	Krios
Voltage (kV)	300
Camera	Gatan K3
Magnification	81,000
Pixel size at detector (Å/pixel)	0.85
Total electron exposure (e ⁻ /Å ²)	55
Frames collected during exposure (no.)	32
Defocus range (µm)	-1.2~-2.2
Automation software	EPU
Micrographs collected (no.)	10,033
Micrographs used (no.)	9,861
Total extract particles (no.)	5,398,065
For each reconstruction	
Refined particles (no.)	734,934
Final particles (no.)	734,934
Point group	C1
Resolution (global, Å)	
FSC 0.5 (unmasked/masked)	4.2/3.4
FSC 0.143 (unmasked/masked)	3.7/3.0
Resolution range (local, Å)	2.8-4.6
Map sharpening B factor (Å ²)	132.6
Map sharpening methods	Half-maps correlation
Model composition	
Protein	1,574
Ligands	7
Model refinement	
Refinement package	PHENIX
- real or reciprocal space	Real Space
- resolution cutoff	3.0
Model-Map scores	
- CC	0.79
B factors (Å ²)	
Protein residues	81.12
Ligands/DNA/RNA	93.25
R.m.s. deviations from ideal values	
Bonds length (Å)	0.003

Bond angles (°)	0.637
Validation	
MolProbity score	1.74
CaBLAM outliers	2.22
Clashscore	8.42
Poor rotamers (%)	1.27
C-beta deviations	0
EMRinger score (if better than 4 Å resolution)	2.51
Ramachandran Plot	
Favored (%)	96.72
Outliers (%)	0

Supplementary Table 2.

List of yeast strains used in this study

pr, promoter

Stain name	Genotype	Background strain	Figure
Wt (BY4741)	<i>MATa his3Δ1 leu2Δ0 met15Δ0 ura3Δ0</i>	<i>MATa</i>	Fig. 1
<i>vtc1Δ</i>	<i>MATa his3Δ1 leu2Δ0 met15Δ0 ura3Δ0 vtc1::KanMX</i>	<i>BY4741</i>	Fig. 1
<i>vtc2Δ</i>	<i>MATa his3Δ1 leu2Δ0 met15Δ0 ura3Δ0 vtc2::KanMX</i>	<i>BY4741</i>	Fig. 1
<i>vtc3Δ</i>	<i>MATa his3Δ1 leu2Δ0 met15Δ0 ura3Δ0 vtc3::KanMX</i>	<i>BY4741</i>	Fig. 1
<i>vtc4Δ</i>	<i>MATa his3Δ1 leu2Δ0 met15Δ0 ura3Δ0 vtc4::KanMX</i>	<i>BY4741</i>	Fig. 1
<i>vtc1Δ vtc2Δ</i>	<i>MATa his3Δ1 leu2Δ0 met15Δ0 ura3Δ0 vtc1::KanMX vtc2::BleoR</i>	<i>vtc1Δ</i>	
<i>vtc2Δ vtc3Δ</i>	<i>MATa his3Δ1 leu2Δ0 met15Δ0 ura3Δ0 vtc2::BleoR vtc3::KanMX</i>	<i>vtc3Δ</i>	Fig. 1
<i>vtc2Δ vtc4Δ</i>	<i>MATa his3Δ1 leu2Δ0 met15Δ0 ura3Δ0 vtc2::BleoR vtc4::KanMX</i>	<i>vtc4Δ</i>	
<i>vtc1</i>	<i>vtc1Δ::KanMX vtc2Δ::BleoR vtc1</i> LEU2-ADHpr-N-2×Strep [pRS415- <i>vtc1</i>]	<i>vtc1Δ vtc2Δ</i>	Fig. 5b
<i>vtc1^{ΔN}</i>	<i>vtc1Δ::KanMX vtc2Δ::BleoR vtc1</i> LEU2-ADHpr-N-2×Strep [pRS415- <i>vtc1^{ΔN}</i>]	<i>vtc1Δ vtc2Δ</i>	Fig. 5b
<i>vtc1^{TM1,mutant}</i>	<i>vtc1Δ::KanMX vtc2Δ::BleoR vtc1</i> LEU2-ADHpr-N-2×Strep [pRS415- <i>vtc1^{TM1,mutant}</i>]	<i>vtc1Δ vtc2Δ</i>	Fig. 5b
<i>vtc3</i>	<i>vtc2Δ::BleoR vtc3Δ::KanMX vtc3</i> LEU2-ADHpr-N-Myc [pRS415- <i>vtc3</i>]	<i>vtc2Δ vtc3Δ</i>	Fig. 5b
<i>vtc3^{TM1,mutant}</i>	<i>vtc2Δ::BleoR vtc3Δ::KanMX vtc3</i> LEU2-ADHpr-N-Myc [pRS415- <i>vtc3^{TM1,mutant}</i>]	<i>vtc2Δ vtc3Δ</i>	Fig. 5b
<i>vtc4</i>	<i>vtc2Δ::BleoR vtc4Δ::KanMX vtc4</i> LEU2-ADHpr-N-2×Strep [pRS415- <i>vtc4</i>]	<i>vtc2Δ vtc4Δ</i>	Fig. 5b
<i>vtc4^{TM1,mutant}</i>	<i>vtc2Δ::BleoR vtc4Δ::KanMX vtc4</i> LEU2-ADHpr-N-2×Strep [pRS415- <i>vtc4^{TM1,mutant}</i>]	<i>vtc2Δ vtc4Δ</i>	Fig. 5b

Supplementary Table 3.

List of primers used in this study

Primer name	Sequence (5'-3')	Remark
Primers for yeast construction		
<i>vtc2</i> Δ (FW)	CAACATAACGACACTTTTTTGACATGGTACAGA AGATTAAGTGAG	<i>vtc2</i> deletion primer
<i>vtc2</i> Δ (Rv)	CTCAGTAGATAGAGTACATATTCTACTTTTGCTC ACATGTTGGTCTC	<i>vtc2</i> deletion primer
KanMX (FW)	CCTCGACATCATCTGCCAGATGCGAAGTTAAG TG	KanMX insert primer
KanMX (Rv)	GTTCTTTGTTGAATTTGTTGTCCACGGCTTCATC GTGTTG	KanMX insert primer
<i>vtc1</i> Δ (FW)	TCGCTATTTTCGGATAGAATGGCAAGAGCGATTA AG	upstream of <i>vtc1</i> gene
<i>vtc1</i> Δ (Rv)	CAGTTTGTGCGTAACCCACGCTTACGATATTG	downstream of <i>vtc1</i> gene
<i>vtc2</i> Δ (FW)	CACTGCGGTATAGCACTTCCAGAAAGATACTGA CTG	upstream of <i>vtc2</i> gene
<i>vtc2</i> Δ (Rv)	CAAAAACCGGAGAAAATGATGTTTATGTAAATG CATTG	downstream of <i>vtc2</i> gene
<i>vtc3</i> Δ (FW)	AAGGCAGAAACGTGGAAACATACACACACGCA CAC	upstream of <i>vtc3</i> gene
<i>vtc3</i> Δ (Rv)	CACCTGCTGAAAGCTGTTTAATATGATTTAATAC	downstream of <i>vtc3</i> gene
<i>vtc4</i> Δ (FW)	TGGTTTGTCTGCGTTTTGACGGAGAGCTACTGA CTTGTAG	upstream of <i>vtc4</i> gene
<i>vtc4</i> Δ (Rv)	GTGTGCGCCTGGTGAAGGTGTGCATTCAGGCA AG	downstream of <i>vtc4</i> gene
<i>vtc1</i> (FW)	CCGCAGTTCGAAAAAGGATCCATGTCTTCAGCA CCATTATTAC	<i>vtc1</i> complement primer
<i>vtc1</i> (Rv)	GACGGTATCGATAAGCTT TTATAACTTAGTGTTAGCGTCATTG	<i>vtc1</i> complement primer
<i>vtc2</i> (FW)	CAAGGATGACGACGATAAGGGATCCATGCTGT TTGGAGTGAAG	<i>vtc2</i> complement primer
<i>vtc2</i> (Rv)	GACGGTATCGATAAGCTTCTAATCACTGCTTGG CCCCATTAACTTG	<i>vtc2</i> complement primer
<i>vtc3</i> (FW)	CGCTCTAGAAGTGGATCCATGGAGCAGAA ACTCATCTCTGAAG	<i>vtc3</i> complement primer
<i>vtc3</i> (Rv)	GACGGTATCGATAAGCTTTTATTCCCAACCAA ATTGAAG	<i>vtc3</i> complement primer
<i>vtc4</i> (FW)	CCGCAGTTCGAAAAAGGATCCATGAAGTTTGG TGAGCACTTG	<i>vtc4</i> complement primer
<i>vtc4</i> (Rv)	GACGGTATCGATAAGCTTTTATTTAGCAACTAG GTTGCAGAAAAAG	<i>vtc4</i> complement primer

<i>vtc1</i> _{K24A/R31A} (FW)	GAGTTGAGCCAGCCGTGTTCTTTGCCAATGAGGC CACCTTTTTGTCTG	<i>vtc1</i> _{K24A/R31A} complement primer
<i>vtc1</i> _{K24A/R31A} (Rv)	CGACAAAAGGTGGCCTCATTGGCAAAGAACACG GCTGGCTCAACTC	<i>vtc1</i> _{K24A/R31A} complement primer
<i>vtc1</i> _{Δ1-21} (FW)	TGGAGCCACCCGCAGTTCGAAAAAATGGAGCCAA AAGTGTCTTTG	<i>vtc</i> _{Δ1-21} complement primer
<i>vtc1</i> _{Δ1-21} (Rv)	CAAAGAACACTTTTGGCTCCATTTTTTCGAACTGC GGGTGGCTCCA	<i>vtc</i> _{Δ1-21} complement primer
<i>vtc3</i> _{K694A/K698A/R705A/R709A} (FW)	AATGCCGGTCTCTGTCGCTGTTGAGGCAGCTGTTTG GCTCGCCAAT	K694A/K698A mutation site
<i>vtc3</i> _{K694A/K698A/R705A/R709A} (Rv)	ATTGGCGAGCCAAACAGCTGCCTCAACAGCGACA GGACCGGCATT	K694A/K698A mutation site
<i>vtc3</i> _{K694A/K698A/R705A/R709A} (FW)	AGTTTGGCTCGCCAATGAAGCCACATTCAATGCCT GGTTAAGTGTAACCAC	R705A/R709A mutation site
<i>vtc3</i> _{K694A/K698A/R705A/R709A} (Rv)	GTGGTTACACTTAACCAGGCATTGAATGTGGCTTC ATTGGCGAGCCAAACT	R705A/R709A mutation site
<i>vtc4</i> _{K622A/R629A} (FW)	GTTCGTGTGGAACCAGCCGTTACTTTGCCACTGA AGCCACCTACCTGTCTTGG	K622A/R629A mutation site
<i>vtc4</i> _{K622A/R629A} (Rv)	CCAAGACAGGTAGGTGGCTTCAGTGGCAAAGTAA ACGGCTGGTTCCACACGAAC	K622A/R629A mutation site

Primers for prokaryotic expression

TTM ₁₈₉₋₄₈₀ ^{Vtc4} (FW)	GAAGGAGATATACATATGGGCAAGCAGCAAAA TTTCGTGAGGCAG	TTM ₁₈₉₋₄₈₀ ^{Vtc4} protein expression and purification
TTM ₁₈₉₋₄₈₀ ^{Vtc4} (Rv)	GTGATGGTGATGCTCGAGCTGGGGCAGCCAAA AGGGGATGGAG	TTM ₁₈₉₋₄₈₀ ^{Vtc4} protein expression and purification
TTM ₁₈₃₋₅₅₃ ^{Vtc3} (FW)	AAGTTGATGCACATATGACCGTGTCCAAGTCCC TGGCTTCCACCAG	TTM ₁₈₃₋₅₅₃ ^{Vtc3} protein expression and purification
TTM ₁₈₃₋₅₅₃ ^{Vtc3} (Rv)	CAGCCGGATCCTCGAGTTACAGGTCGGGCAGC CAAAAGGGCAG	TTM ₁₈₃₋₅₅₃ ^{Vtc3} protein expression and purification
TTM ₁₈₉₋₄₈₀ ^{Vtc4,m} utant (FW)	GAAGGCCAGGTTTGCCCTGGCCGAGGCCACG TGAATGAC	K300A/R302A mutant point

TTM ₁₈₉₋₄₈₀ ^{Vtc4,m} utant (Rv)	GTCATTCACGTGGGCCTCGGCCAGGGCAAACCT GGCCTTC	K300A/R302A mutant point
TTM ₁₈₉₋₄₈₀ ^{Vtc4,m} utant (FW)	CCAGGTGTTTGCCGCCATGAGAAAGGAGGGCA AGAAG	K320A mutation site
TTM ₁₈₉₋₄₈₀ ^{Vtc4,m} utant (Rv)	CTTCTTGCCCTCCTTTCTCATGGCGGCAAACAC CTGG	K320A mutation site
TTM ₁₈₃₋₅₅₃ ^{Vtc3,m} utant (FW)	ATCGGCAAGCTGCTGGACGCCCCCGATATCTTT CTGGAG	K333A mutation site
TTM ₁₈₃₋₅₅₃ ^{Vtc3,m} utant (Rv)	CTCCAGAAAGATATCGGGGGCGTCCAGCAGCT TGCCGAT	K333A mutation site
TTM ₁₈₃₋₅₅₃ ^{Vtc3,m} utant (FW)	GGAGATCAGACTGCAGATGGCCGCTGCCTTTAT CAACAATTTTCATC	K362/364A mutation site
TTM ₁₈₃₋₅₅₃ ^{Vtc3,m} utant (Rv)	GATGAAATTGTTGATAAAGGCAGCGGCCATCT GCAGTCTGATCTCC	K362/364A mutation site
TTM ₁₈₃₋₅₅₃ ^{Vtc3,m} utant (FW)	GACCCTAGCTACAAGAACTTCCTGATCAACCAG CTGAG	Y380F mutation site
TTM ₁₈₃₋₅₅₃ ^{Vtc3,m} utant (Rv)	CTCAGCTGGTTGATCAGGAAGTTCTTGTAGCTA GGGTC	Y380F mutation site

Primers for eukaryotic expression

Vtc1 (FW)	ATTATCGATCCGGAGGTACCATGGCTTCCTCCGC CCCCCTG	VTC1 protein expression and purification
Vtc1 (Rv)	ATGGGTAGGCGCTCTCGAGCAGCTTGGTATTGG CATC	VTC1 protein expression and purification
Vtc3 (FW)	GATGACGACGATAAGGGATCCATGCTGTTTGGC ATCAAGCTG	VTC3 protein expression and purification
Vtc3 (Rv)	CTGCTAGCAAGCTTCTCGAGTTACTCGCCCACC AGGTAAAG	VTC3 protein expression and purification
Vtc4 (FW)	ATTATCGATCCGGAGGTACCATGGCTAAGTTCGG CGAGCAC	VTC4 protein expression and purification
Vtc4 (Rv)	GGCTCCAGGCGCTCTCGAGCTTGGCCACCAGGT TAC	VTC4 protein expression and purification
Vtc4 _{R264A/R266A/ E426N} (FW)	GAGGCCACGCCCTGGCGTGGTACGGCGGCA TG	R264A/R266A mutation site
Vtc4 _{R264A/R266A/ E426N} (Rv)	CATGCCGCCGTACCACGCCAGGGCGTGGGCCT C	R264A/R266A mutation site

Vtc4 _{R264A/R266A/} E426N (FW)	TACGCCGTGCTGAACGTGAAGCTGCAGACCCA G	E426N mutation site
Vtc4 _{R264A/R266A/} E426N (Rv)	CTGGGTCTGCAGCTTCACGTTACAGCACGGCGTA	E426N mutation site
Vtc3 _{Y22F/K26A/K1} 30A (FW)	GATTCCTACATCGACTTCGAGAGGCTGGCTAAG CTGCTGAAGGAG	Y22F/K26A mutation site
Vtc3 _{Y22F/K26A/K1} 30A (Rv)	CTCCTTCAGCAGCTTAGCCAGCCTCTCGAAGTC GATGTAGGAATC	Y22F/K26A mutation site
Vtc3 _{Y22F/K26A/K1} 30A (FW)	TTCATCAAGATCGTGAAGGCTCACGATAAGCTG CAC	K130A mutation site
Vtc3 _{Y22F/K26A/K1} 30A (Rv)	GTGCAGCTTATCGTGAGCCTTCACGATCTTGAT GAA	K130A mutation site
Vtc4 _{Y22F/K26A/K1} 33A (FW)	TACTACTACATCTCCTTCGACGACCTGGCTACA GAGCTGGAGGAC	Y22F/K26A mutation site
Vtc4 _{Y22F/K26A/K1} 33A (Rv)	GTCCTCCAGCTCTGTAGCCAGGTCGTCGAAGGA GATGTAGTAGTA	Y22F/K26A mutation site
Vtc4 _{Y22F/K26A/K1} 33A (FW)	CCAGAAGATCATCAAGGCTCACGATAAGAAGA CAG	K133A mutation site
Vtc4 _{Y22F/K26A/K1} 33A (Rv)	CTGTCTTCTTATCGTGAGCCTTGATGATCTTCTG G	K133A mutation site
Vtc3 _{K126A/K129A/} K133A (FW)	GGCTTCATCGCTATCGTGGCTAAGCACGATGCT CTGCACCCCA	Vtc3 _{K126A/K129A/K1} 33A protein expression and purification
Vtc3 _{K126A/K129A/} K133A (Rv)	TGGGGTGCAGAGCATCGTGCTTAGCCACGATA GCGATGAAGCC	Vtc3 _{K126A/K129A/K1} 33A protein expression and purification
Vtc4 _{K129A/K132A/} K136A (FW)	GGCTTCCAGGCCATCATCGCCAAGCACGATGCC AAGACAG	Vtc4 _{K129A/K132A/K1} 36A protein expression and purification
Vtc4 _{K129A/K132A/} K136A (Rv)	GGCTTCCAGGCCATCATCGCCAAGCACGATGCC AAGACAG	Vtc4 _{K129A/K132A/K1} 36A protein expression and purification
Vtc1 _{K24A/R31A} (FW)	AGAGTGGAGCCTGCCGTGTTCTTCGCCAATGAG GCCACCTTTCTGTCCTG	Vtc1 _{K24A/R31A} protein expression and purification
Vtc1 _{K24A/R31A} (Rv)	CAGGACAGAAAGGTGGCCTCATTGGCGAAGAA CACGGCAGGCTCCACTCT	Vtc1 _{K24A/R31A} protein

		expression and purification
		Vtc1 $_{\Delta 1-21}$
Vtc1 $_{\Delta 1-21}$ (FW)	ATTATCGATCCGGAGGTACCATGGAGCCTAAG GTGTTCTTCGCCAAT	protein expression and purification
		Vtc1 $_{\Delta 1-21}$
Vtc1 $_{\Delta 1-21}$ (Rv)	ATGGGTAGGCGCTCTCGAGCAGCTTGGTATTGG CATC	protein expression and purification
Vtc3 $_{K694A/K698A/R705A/R709A}$ (FW)	GAACGCCGGACCTGTGGCTGTGGAGGCTGCTG TGTGGCTGGCTAATG	K694/R698A mutation site
Vtc3 $_{K694A/K698A/R705A/R709A}$ (Rv)	GATGAAATTGTTGATAAAGGCAGCGGCCATCT GCAGTCTGATCTCC	K694/R698A mutation site
Vtc3 $_{K694A/K698A/R705A/R709A}$ (FW)	TGTGGCTGGCTAATGAGGCTACCTTCAATGCTT GGCTGAGCGTGACAAC	R705/R709A mutation site
Vtc3 $_{K694A/K698A/R705A/R709A}$ (Rv)	GTTGTCACGCTCAGCCAAGCATTGAAGGTAGCC TCATTAGCCAGCCACA	R705/R709A mutation site
		Vtc4 $_{K622A/R629A}$
Vtc4 $_{K622A/R629A}$ (FW)	GTGAGAGTGGAGCCCCGCGTGTACTTTGCCACC GAGGCCACATACCTGAGCTGG	protein expression and purification
		Vtc4 $_{K622A/R629A}$
Vtc4 $_{K622A/R629A}$ (Rv)	CCAGCTCAGGTATGTGGCCTCGGTGGCAAAGT ACACGGCGGGCTCCACTCTCAC	protein expression and purification
		VTC1
		background
Vtc1 $_{C105M}$ (FW)	GGACCTACACTGCTGATGTTTTTCCTGCTGGTG	Cys mutation
		VTC1
VTC1 $_{C105M}$ (Rv)	CACCAGCAGGAAAAACATCAGCAGTGTAGGTC C	background
		Cys mutation
		VTC3
Vtc3 $_{C106M}$ (FW)	GAACACCCTGGAGGAGATGCTGGATGAGGCTC AGAG	background
		Cys mutation
		VTC3
Vtc3 $_{C106M}$ (Rv)	CTCTGAGCCTCATCCAGCATCTCCTCCAGGGTG TTC	background
		Cys mutation
		VTC3
Vtc3 $_{C751M}$ (FW)	CTTTCTGACCCTGTTTCATGGGCGTGTGGGCTTA C	background
		Cys mutation
		VTC3
Vtc3 $_{C751M}$ (Rv)	GTAAGCCCACACGCCCATGAACAGGGTCAGAA AG	background
		Cys mutation

		VTC4
Vtc4 _{C63M} (FW)	AAGGTGTACACATTCATGAAGGTGAAGCACAG CGAGGTG	background Cys mutation VTC4
Vtc4 _{C63M} (Rv)	CACCTCGCTGTGCTTCACCTTCATGAATGTGTA CACCTT	background Cys mutation VTC4
Vtc4 _{C418M} (FW)	GATGATAAGGATATCATGAGGTTCCCCTACGCC GTG	background Cys mutation VTC4
Vtc4 _{C418M} (Rv)	CACGGCGTAGGGGAACCTCATGATATCCTTATC ATC	background Cys mutation VTC4
Vtc4 _{C614M} (FW)	CCGGCAAGACCATCATGGTGCCTGTGAGAGTG GAG	background Cys mutation VTC4
Vtc4 _{C614M} (Rv)	CTCCACTCTCACAGGCACCATGATGGTCTTGCC GG	background Cys mutation VTC4
Vtc4 _{C716M} (Rv)	GGCTCCAGGCGCTCTCGAGCTTGGCCACCAGGT TCATGAAAAAGC	background Cys mutation
Vtc4 _{K415C} (FW)	CTTTTAAGCAGCTGGATGATTGTGATATCTGTA GGTTCCCCTACGCC	K415C mutation site
Vtc4 _{K415C} (Rv)	GGCGTAGGGGAACCTACAGATATCACAATCAT CCAGCTGCTTAAAAG	K415C mutation site
Vtc4 _{R689C} (FW)	GGGTGGTGAACATCAGGCTGAAGTGTGCCGTG GATTACGAGGATAAGATC	R689C mutation site
Vtc4 _{R689C} (Rv)	GATCTTATCCTCGTAATCCACGGCACACTTCAG CCTGATGTTACCACCC	R689C mutation site

Supplementary References

- 1 Aschar-Sobbi, R. et al. High sensitivity, quantitative measurements of polyphosphate using a new DAPI-Based approach. *Journal of Fluorescence* **18**, 859-866 (2008).
- 2 Hothorn, M. et al. Catalytic Core of a Membrane-Associated Eukaryotic Polyphosphate Polymerase. *Science* **324**, 513-516 (2009).
- 3 Wild, R. et al. Control of eukaryotic phosphate homeostasis by inositol polyphosphate sensor domains. *Science* **352**, 986-990 (2016).
- 4 Smart, O. S., Neduvilil, J. G., Wang, X., Wallace, B. A. & Sansom, M. S. P. HOLE: A program for the analysis of the pore dimensions of ion channel structural models. *Journal of Molecular Graphics & Modelling* **14**, 354-360 (1996).
- 5 Schwieters, C. D., Bermejo, G. A. & Clore, G. M. Xplor-NIH for molecular structure determination from NMR and other data sources. *Protein Science* **27**, 26-40 (2018).